STRAIN LOCALIZATION IN IRRADIATED MATERIALS

THAKSANG BYUN* and NAOYUKI HASHIMOTO[1]
Materials Science and Technology Division, Oak Ridge National Laboratory
Oak Ridge, TN 37831, USA,
[1]Department of Applied Science and Engineering, Hokkaido University
N13, W8, Kita-ku, Sapporo 060-8628, Japan
*Corresponding author. E-mail : byunts@ornl.gov

Received August 19, 2006

Low temperature irradiation can significantly harden metallic materials and often lead to strain localization and ductility loss in deformation. This paper provides a review on the radiation effects on the deformation of metallic materials, focusing on microscopic and macroscopic strain localization phenomena. The types of microscopic strain localization often observed in irradiated materials are dislocation channeling and deformation twinning, in which dislocation glides are evenly distributed and well confined in the narrow bands, usually a fraction of a micron wide. Dislocation channeling is a common strain localization mechanism observed virtually in all irradiated metallic materials with ductility, while deformation twinning is an alternative localization mechanism occurring only in low stacking fault energy(SFE) materials. In some high stacking fault energy materials where cross slip is easy, curved and widening channels can be formed depending on dose and stress state. Irradiation also prompts macroscopic strain localization (or plastic instability). It is shown that the plastic instability stress and true fracture stress are nearly independent of irradiation dose if there is no radiation-induced phase change or embrittlement. A newly proposed plastic instability criterion is that the metals after irradiation show necking at yield when the yield stress exceeds the dose-independent plastic instability stress. There is no evident relationship between the microscopic and macroscopic strain localizations; which is explained by the long-range back-stress hardening. It is proposed that the microscopic strain localization is a generalized phenomenon occurring at high stress.

KEYWORDS : Radiation Effects, Localized Deformation, Dislocation Channeling, Deformation Twinning, Strain Hardening

1. INTRODUCTION

Irradiation with energetic particles hardens metallic materials by producing numerous defect clusters and makes them more prone to microscopic and macroscopic strain localizations and embrittlement [1-4]. Since these phenomena are the main degradation mechanisms of nuclear structural materials in low-temperature environments, a number of studies have been attempted to find the detailed mechanisms and their relationships to the macroscopic material behaviors [5-24]. Even though the microscopically-localized deformation has been well-known for decades and observed in virtually all irradiated metallic materials, much of the detailed mechanisms and their effects on macroscopic mechanical behaviors have never been fully understood [20-24]. Strain localization and embrittlement are among the major concerns in designing future nuclear facilities, where much higher displacement-per-atom (dpa) damage is expected than in conventional power plant components. The lifetime doses of several tens to hundreds of dpa are predicted for advanced nuclear applications, such as spallation neutron source vessels, fusion reactor first walls, and fuel claddings of fast reactors, for a year or their life times [25], while relatively low damage (< 0.1 dpa) is predicted for the pressure vessel steels of current water-cooled power reactors after the end of life. Most of the commercial structural alloys will show embrittlement as well as plastic instability at those high doses. It is necessary, therefore, to understand those irradiation-induced degradation phenomena in materials for successful design and operation of those future devices.

Since the earlier studies during the sixties to eighties of last century [1,4-13], the dislocation channel, which is formed by clearance of radiation-induced defects, has been the icon of the localized deformation in irradiated materials. Actually, those earlier studies have found most of the important features of dislocation channeling such as the defect-cleared channels, speed of formation, dimensions of channels, and some defect clearing mechanisms [7-13]. In the past decade research efforts to elucidate the localized deformation and related mechanisms have been largely renewed because of advanced electron microscopy skills,

higher computer capacities for simulations, and new theoretical models [26-38]. However, details of the mechanism, like the one for channel initiation, have not been fully understood: no complete theoretical method to predict the critical stress for channeling in the commercial nuclear materials has been proposed, although it can be an important parameter for material selection and design purposes [7,24,37].

In low stacking fault energy materials, such as 300 series austenitic stainless steels, the mechanical twinning is an alternative microscopic localization mechanism to the dislocation channeling [37-46]. Twinning has been recognized as a localization mechanism because it is also formed by massive but confined dislocation glides [37,45]. Often, both dislocation channeling and deformation twinning take part in the deformation of low-temperature irradiated stainless steels [3,36,37]. Both mechanisms require significantly high stresses to initiate, and in most metallic materials irradiated at low temperatures (<~200 °C) those strain localizations occur above ~10^{-2} dpa [37,38].

Plastic instability (or necking) is the macroscopic version of strain localization. In most of the body-centered cubic (bcc) and hexagonal close-packed (hcp) metals, prompt necking at yield almost always occurs after low temperature irradiation to a dose higher than 0.1 dpa [1,3,13-15, 18-21]. Thus far, this has led to a common belief that the plastic instability and whole macroscopic strain-hardening behavior are connected to the change of microscopic deformation mechanism from uniform to localized deformation. In recent studies, however, no evident relationship between the microscopic and macroscopic strain localizations was found when the stress-strain behaviors were compared in terms of true stress units, although significant changes in engineering flow curves and deformation mechanisms were observed [47-51]. Further, the prompt necking at yield is not observed in some high purity bcc and many face-centered cubic (fcc) materials until the irradiation dose reaches a few or tens of dpa. This might be because of their high strain-hardening rates and delayed clustering of point defects to larger defects. The true stress analyses led to a few new findings: the metals after irradiation showed necking at yield when the yield stress exceeded the true plastic instability stress for the unirradiated material; both the plastic instability stress and the true fracture stress were nearly independent of dose if no radiation-induced phase change or embrittlement exists [50,51].

This paper aims to provide a summary for the state-of-the-art understandings on the strain localization phenomena and the relationship between the microscopic mechanisms and the macroscopic behaviors. First, the channeling and twinning in irradiated materials will be reviewed and summarized. Second, the strain-hardening behavior and macroscopic strain localization, or necking deformation, will be discussed focusing on the dose dependence of true stress-true strain curves and true stress parameters. Third, the relationships between those macro- and micro-behaviors will be discussed; the latest findings through theoretical analysis will be introduced. The last part of this paper will be a generalization of the strain localization phenomenon. In this paper supporting data are provided in figures and tables and represent recent studies at ORNL [3,36-38,41-51].

2. MICROSCOPIC STRAIN LOCALIZATION

2.1 Dislocation Channeling

2.1.1 General Features

As known for decades, the dislocation channeling is a process of heterogeneous plastic deformation by ordinary dislocations, in which dislocations released from a source glide along a limited number of slip planes, removing or cutting through small barriers in their paths [1-14]. This defect-clearing interaction creates an easy path for subsequent dislocation glide and a narrow channel that is a fraction of a micron wide is developed. It has been observed that the strain in a channel reaches a few hundred percent at a bulk strain of a few percent [1-4,8,11,37]. Actually, the channeling process was predicted by Cottrell [52] even before the first transmission electron microscope (TEM) observation was reported. He proposed that slip dislocations could sweep away defect clusters, facilitating the easier passage of subsequent glides on the cleared planes. Many of the earliest experimental observations of dislocation channeling were for neutron-irradiated single crystals of copper or copper alloys [5-8,11].

Although the initiation mechanism for channeling process cannot be recorded because it is a high speed process, details on the channeled microstructures have been well-characterized by TEM techniques. One of the most systematic studies among the earliest studies in 1960s [6-10] was Sharp's work for single crystalline copper after irradiation to ~10^{-3} dpa [8], where the width of channels were measured in TEM as a function of temperature, dose, and strain. The width and spacing of the channels were compared with the data by surface replica technique. Some details observed in channeled copper single crystals [8] are listed as follows:

A. The shear strain was well-confined in narrow bands; the grown-in dislocations between slip bands showed no sign of having moved and were heavily jogged; they became jogged by sinking irradiation produced defects.
B. The defect-free channels were parallel to the easy-glide trace of a {111} plane, whose width was constant along their length although different channels had slightly different widths (mean width = 0.15 micrometers).
C. Although patches of dislocation debris were observed within channels, channels were clear of (almost) all defects of visible size and no piling up of defects at the side of the channel was found.
D. The channel width and step height at specimen surface

decreased with decreasing test temperature; the channel width decreased with increasing dose while the step height increased with dose. Effects of thermal annealing on deformation were similar to the effects from a reduction of dose.

E. The channel width was independent of strain rate in room temperature deformation (0.1 and 0.001 in/min). Also, the channel width for large strains was about the same as that for small strains, although spacing decreased with strain.

F. Cross slip channels were commonly observed after deformation at room temperature, but rarely at 77K. The channels became more irregular at 200 °C, at which the slip was a combination of primary and cross slip.

G. Intersection of slip line showed that the shear within a channel was fairly evenly distributed across the channel. The debris from work hardening within channel distributed evenly.

These microstructural details led to a description for the whole process of channeling consisted of initiation, dislocation multiplication, softening, and work hardening stages [8]. Also, other studies confirm that the characteristics of channels observed in copper, a typical fcc metal, are not significantly different from those of the materials with other crystal types [10,12-14], except that the shape of channels, straightness in particular, is affected by stacking fault energy [38].

For work hardening within channel band or for termination of channeling process, the long-range stress from pileup dislocations is considered to be the most important factor [7,11]. Since some hard obstacles like aluminum-oxide (Al_2O_3) particles can introduce a long-range stress hardening by Orowan mechanism, which compensates the softening effect from the clearance of defect clusters, the tendency to form channels is reduced in such particle-hardened materials. Sharp's experimental results [11] showed that cleared channels were formed in Cu-0.8%Co and internally oxidized Cu-0.05%Al single crystals, whereas the dislocations were just confined to a few slip planes in internally oxidized Cu-4%Al single crystals, where oxide particles were abundant, without forming cleared channels. Since other hardening mechanisms are expected to have minimal role in the cleared channels, the above evidence suggests that the buildup of long-range stress will be a main hardening mechanism in the channeling process. As will be discussed separately later, the long-range back stress from pileup dislocations is the main hardening stress in both polycrystalline and single-crystalline materials [7-24]. Polycrystalline materials, where higher back-stress hardening is expected because of pileups against grain boundaries, might show narrower channels than in single crystals.

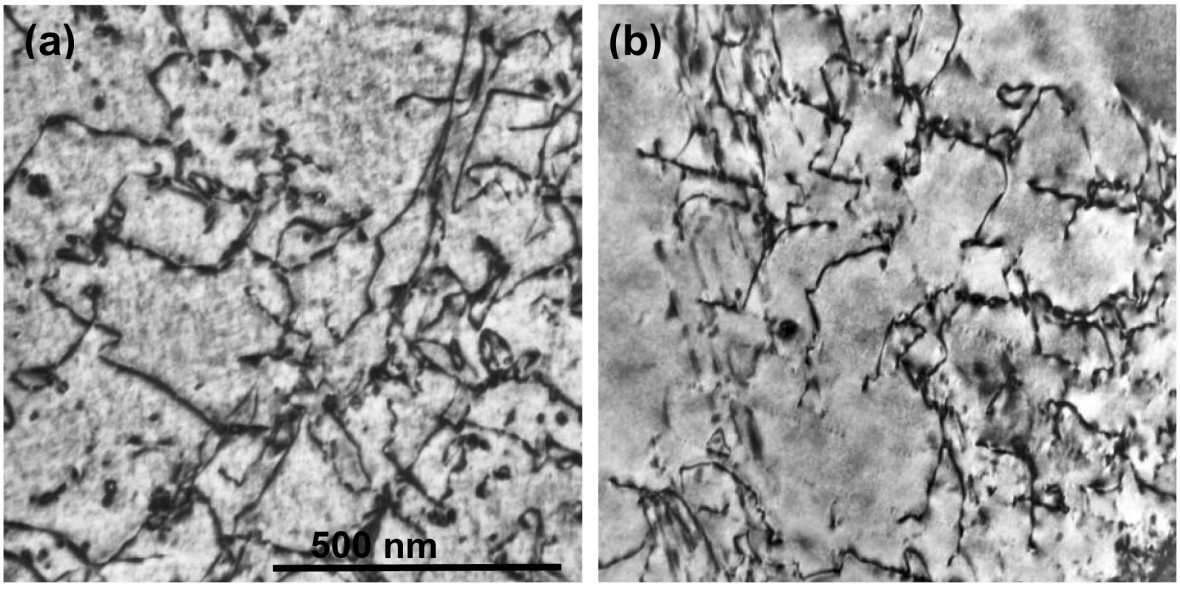

Fig. 1. Uniform Deformation Microstructures (random dislocation tangles) Found in (a) Pure Vanadium (bcc) at 10% Strain and in (b) 316 Stainless Steel (fcc) at 6%. Both were Deformed by Uniaxial Tensile Load at Room Temperature [3,36]

2.1.2 Latest Results at ORNL

Characterizing and mapping strain localization for selected commercial and pure metals have been pursued at ORNL for in recent years. Examples for uniform (random) and channeled microstructures are presented in Figs. 1 and 2, respectively, where dramatic differences are found in the features of residual dislocations and glide tracks. In Figs. 1(a) and 1(b) are the TEM microstructures after

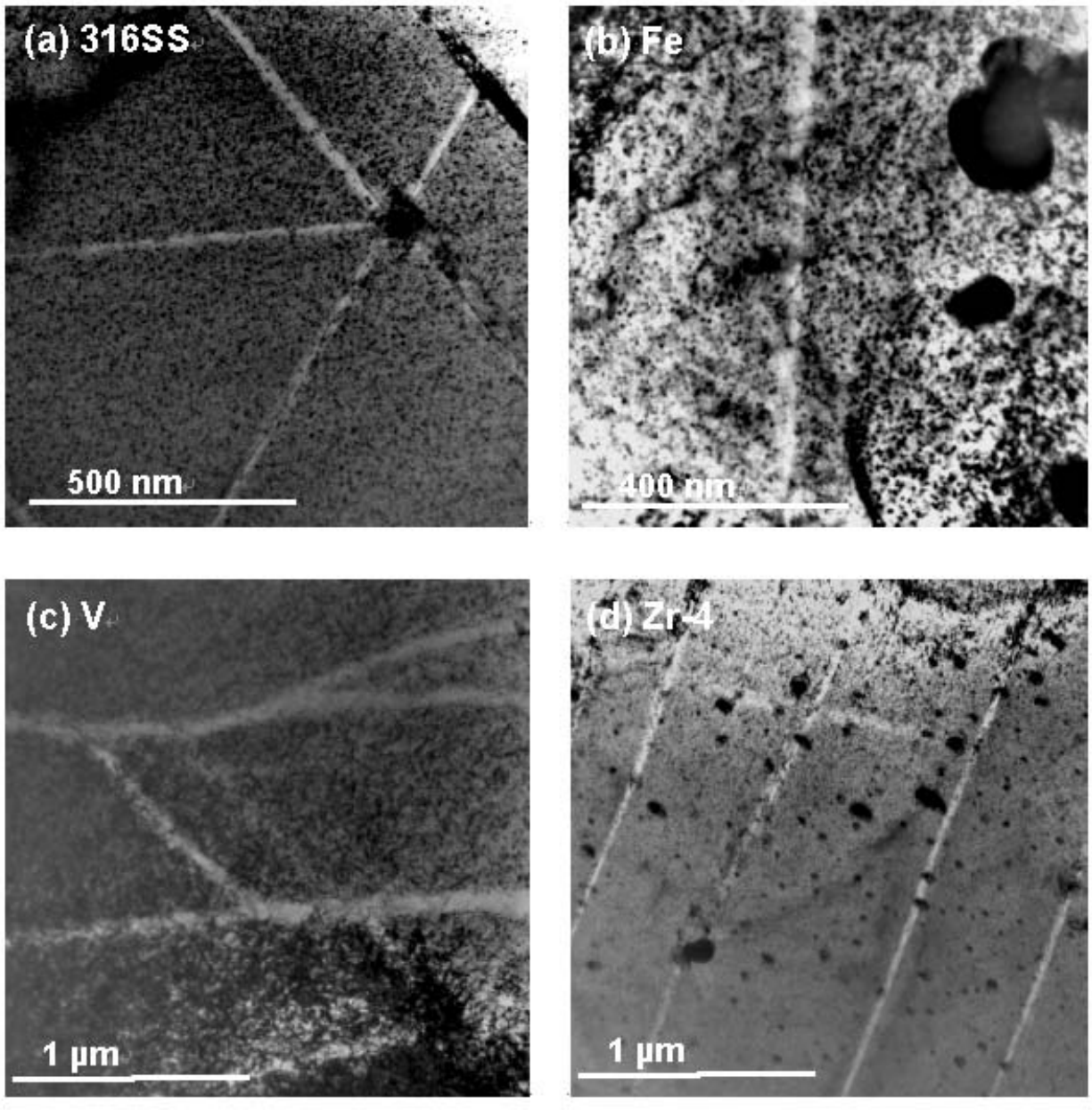

Fig. 2. Channeled Microstructures After Neutron Irradiation at ~80 ℃ and Deformed at Room Temperature [3,38]: (a) Straight Channels and their Interception in 316 Stainless Steel at 0.78 dpa, 5% Strain; (b) Single Channel in Iron at 0.89 dpa, 0.2% Nominal Strain; (c) River-pattern Channel Network in Vanadium at 0.69 dpa, 10% Strain; (d) Parallel Channels in Zr-4 at 0.8 dpa, 6% Strain. The Vanadium Specimen was Deformed by Disk-bend Technique, while the Others were Deformed by Uniaxial Tensile Loading

the uniform deformation in unirradiated vanadium and 316 stainless steel. Both are annealed materials. The random distributions of residual dislocations indicate that dislocation glides have not been confined in any bands and dislocations have freely interacted with each other during deformation. Comparison of the displacement made by residual dislocations with the bulk strain measured can confirm that most of the dislocations contributing to plastic strain have glided to the specimen surfaces. No track has been left in these unirradiated specimens without visible defect clusters.

As presented in Fig. 2, channeling is largely favored in the room temperature deformation after low-temperature neutron irradiation [3]. In the channeled microstructures of 316 stainless steel, Fig. 2(a), the defect-cleared channels formed on {111} planes intercept each other and divide the deformation microstructure into blocks with little dislocation activity in the unchanneled matrix. It is known that the active {111}<110> slip systems for channeling are the same as those with uniform deformation [1-4]. With an average of 1 to 3 dislocations glided on each slip plane in the channel [6-12], shear strain is well confined in the channel and uniformly distributed through the width [3,8,11]. Although the secondary slip was active during the channel deformation, and therefore formed many crossings with the primary slip bands, no primary or secondary channel segment exhibited curvature in the low SFE fcc materials [8,11,37-46].

In A533B steel, a quenched and tempered bcc material that has very fine composite structure of carbides and laths, observation of channels is difficult, and therefore the channeled microstructure has seldom been reported [3]. This is because such a low uniform ductility material shows a prompt necking at yield at a low dose, just above ~0.01 dpa, however, channeling occurs above ~0.1 dpa. Therefore, taking TEM samples from the necked specimen is extremely difficult. This difficulty is also because channeling seems to be delayed to a higher dose due to the high internal stress generated in such a fine, complex microstructure. A straight channel in neutron-irradiated A533B steel is presented in Fig. 2(b). This was obtained from the uniform section of a specimen that showed prompt necking at yield, thus the corresponding bulk plastic strain was merely about 0.2%.

Although most of the channels reported for metallic materials are straight, narrow bands with constant width, some materials develop curved channels, sometimes with widening as they propagate [3,18,36]. A physical parameter that controls the channel shape is believed to be the stacking fault energy. The SFE is also believed to determine the mechanism of strain localization. In irradiated austenitic stainless steels, typical low SFE materials, both twinning and channeling mechanisms are operative, depending on the type of defect clusters and on testing condition [3,37,45, 46]. One of the high SFE materials is bcc vanadium. Recent study on channeling by Hashimoto et al. [36,38] shows that the tendency for channeling increased gradually with dose. Plastic deformation was weakly channeled at 0.012 dpa; most of the remaining dislocations are confined within the band, and the boundary with the surrounding undeformed matrix is vague. It is believed that a dose of 0.01 dpa is about the critical dose for channeling in pure vanadium. Most of the dislocations and pileups within the localized bands disappeared in the channels formed at a higher dose of 0.12 dpa [36]. Fig. 2(c) presents a channel network in vanadium after neutron-irradiation to 0.69 dpa and disk bend deformation to 10% strain. This channel network is analogous to the river pattern in the cleavage surfaces of bcc metals; the channels split, merge, widen, and curve during propagation. It was observed that the channel width in the widest part was larger than 200 nm, which was about 4 times larger than that of the narrowest side, about 50 nm [38]. Only a perfect screw dislocation can change its slip plane by cross slip, in which its Burgers vector is not changed [53-55]. Since one cross slip onto another slip plane will make just a sharp deflection in the path of a dislocation, the curving and/or widening over a large area, as seen in Fig. 2(c), must result from numerous cross slips. A curved path can be formed by multiple cross slips per each dislocation or by cross slips on successive planes at different positions with single cross slip per each dislocation.

The easy glide plane in a crystalline material is usually the most closely-packed plane [55]. In contrast to the fcc lattice where the {111} slip planes predominate, bcc crystals commonly deform by slip on {110}, {112} and {123} planes [29]. These planes have similar atom packing density and include <111> glide directions. Dislocation channels in an irradiated material are known to form in the same slip systems as individual dislocation glide in the unirradiated material [1-4,8,11,36]. TEM micrographs of bcc vanadium show that channels in vanadium are formed primarily on {112} planes with a few exceptions in which channels are formed on {110} or {123} planes [36,38]. No stacking fault or dissociated dislocation was observed because the stacking fault energy of vanadium is too high to dissociate dislocations.

No significantly different feature is found in the channels formed in the hexagonal close packed (hcp) material Zr-4 [3]. Fig. 2(d) displays nearly parallel channels formed after neutron irradiation to 0.8 dpa. At lower doses the channel edges were not sharp, and the channel contrast was not strong, suggesting that there were some remnants of defect clusters. The dislocation channels became obvious at or above 0.1 dpa. In Fig. 2(d) the dislocation slips tend to occur only on one prismatic $\{10\bar{1}0\}\langle 11\bar{2}0\rangle$ system, and cross channels were rare. The major channels were nearly uniformly 40-75 nm wide and were spaced at 400-1100 nm. The pyramidal $\{10\bar{1}1\}\langle 11\bar{2}0\rangle$ slip system was found only at lower doses [3].

Other important observation is the existence of dense grown-in dislocations in vanadium formed by irradiation [38]. Fig. 2(c) shows that these dislocations were removed by channeling process, as were the black-dot defects. Some

dislocations observed within the channels are believed to be extended parts of grown-in dislocations from the non-channeled area.

2.2 Deformation Twinning

Deformation twinning is preferred in the materials with unremovable obstacles which can induce high stress because its initiation requires higher local stress within the twin band [37,45,46]. The deformation twinning which is often observed in low SFE fcc materials is classified as a strain localization mechanism because of its nature of massive dislocation glide in narrow bands [1-3]. Figs. 3(a)

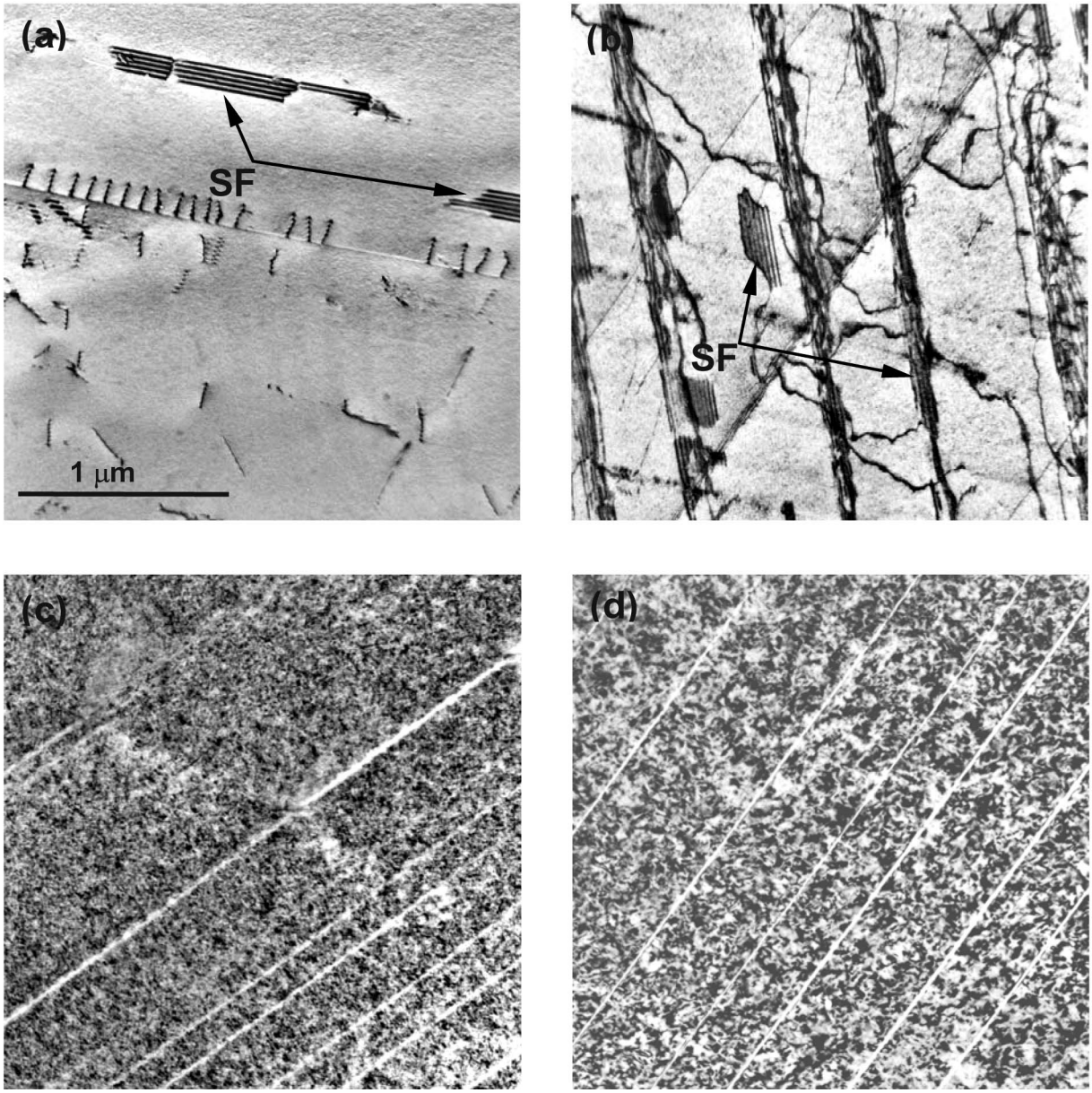

Fig. 3. Microstructures of 316LN Stainless Steel After Irradiation with 350 keV Helium Ions at 200 ℃, Followed by Room Temperature Deformation to About 10% Strain by Disk-bend Technique [46]. Corresponding Doses are (a) 0.015 dpa, (b) 0.15 dpa, (c) 1.5 dpa, and (d) 15 dpa. Stacking Faults (SF) are Found at the two Lower Doses; while Only Deformation Twins are Found at Higher Doses. Very Thin Twins also Exist in (b). $\bar{Z}(zone\ axis) \approx [110]$

to 3(d) display a progressive localization in 316LN stainless steel after helium-ion irradiation up to 15 dpa (20 at.% He) and deformation to a plastic strain of about 10% at room temperature. As an indication of dissociation of perfect dislocations, the stacking fault segments (indicated by SF) are seen at 0.015 and 0.15 dpa. These stacking fault segments are formed by dissociation of perfect dislocations (Burgers vector = $a/2$ <110> type, where a = lattice parameter) into Shockley partial dislocations ($a/6$ <112> type). At 0.015 dpa, Fig. 3(a), the glide dislocations became confined on {111} planes forming pile-ups. Some of the pile-up dislocations are dissociated into Shockley partials forming multiple stacking faults in a row on the same plane. As the irradiation dose increased, the separation of Shockley partials or the width of stacking faults became larger. At 0.15 dpa, Fig. 3(b), the fringes extended over the whole grain, which appear as long stacking fault strips or thin twins. Cross-slip seemed to be severely restricted during deformation at 0.15 dpa and dislocation glide occurred mostly on {111} slip planes. Patches of stacking fault fringes became evident along the {111} glide planes and glide of partials on successive planes formed thin twin layers [41-43]. Some random dislocations are still found in Fig. 1(b). The deformation bands consist of stacking faults/twin layers and perfect and partial dislocations and they formed on at least three slip systems on {111} planes.

In Fig. 3 a dose of 0.15 dpa seems to be a threshold for the transition of deformation microstructure. The separation between leading and trailing partials became infinite or large enough to cover a whole grain, which was usually coincident with twinning dominant. At higher doses, 1.5 and 15 dpa, the propensity for separated partials increased dramatically and the faulted regions on adjacent glide planes began to overlap or glide of partial dislocations occurred on successive planes forming twin bands as white, straight bands in edge-on view, as seen in Figs. 3(c) and 3(d). The twin bands at the highest dose of 15 dpa have clearer boundaries with the matrix [41-43].

In general, the plastic deformation was progressively localized on {111} slip planes with increasing dose, as the ability to cross-slip became increasingly discouraged by the increase of the separation distance of Shockley partial dislocations [44-46]. Consequently, the deformation microstructure changed from a dislocation network dominant to twin dominant microstructure with increasing radiation dose. Because of the low SFE, the straightness of localized bands is retained even under a complex loading. Bend loading by a ball puncher, used for producing Figs 3(a) to 3(d), can generate a multiaxial, high constraint stress state within a disk specimen [44]. Deformation in a punched (bent) disk under multiaxial stress fields should increase the possibility of cross slip in dislocation glide due to geometrical requirements. In the deformation microstructures of stainless steel, however, the effect of this complex stress state was not observed, as shown in Fig. 3. Only straight bands were formed in all localized deformations.

It may be also an important finding that there exists a transition range of dpa dose in the shift of deformation mechanism from random dislocation networks to twins, in which the separation of partials increases with increasing dose [46]. At room temperature this transition range covered a dose range 0 to 0.15 dpa. In the twin-dominant microstructures, the distance between twin bands is typically a fraction of a μm.

2.3 Critical Stress for Strain Localization

2.3.1 Channeling Stress

Although the channeling phenomenon has been observed in many materials to establish its general features as described in section 2.1 [1-4,6-13] and some mechanisms for dislocation-defect interactions or defect clearing processes have been observed and proposed [26-35], the criterion for the phenomenon has not been clearly determined [46].

A model based on lattice hardening and dislocation pileup, as a first theoretical model for channeling, was proposed by Makin and Sharp [7] to explain the channel formation in irradiated copper single crystals, in which the critical stress to form a channel is the stress to generate the first dislocation loop in the environment of the defect clusters [7]. As the slipped area expands, a pile-up forms, and the stress required to expand this pile-up falls. Under a constant load the pile-up rapidly increases in size and hence slip lines form quickly. This high speed formation has been confirmed by cinephotography on the slip line formation at the specimen surface: slip lines were formed in less than one microsecond. This study also indicates that the yielding process in irradiated materials is similar to the localized, heterogeneous deformation that occurs during the formation of Lüders bands in hardened materials [3,55].

In the Makin and Sharp's model [7], however, the role of grain boundaries or other harder obstacles was not explored, and consequently it produced ever-decreasing stress with the pileup expansion. This decreasing local stress cannot explain the high strain-hardening rate and formation of multiple channels, which indicates termination of a channel and initiation of the next channel in a different area, even in a single crystal specimen. To explain channeling in polycrystalline materials, therefore, an integrated process of dislocation pileup against the grain boundary and subsequent propagation to adjoining grains should be considered. At a critical stress, the pileup dislocations can unlock a source in the adjoining grain or the pileup loop can expand to larger volume [55]. Since details in channeling processes, such as dislocation generation and interaction with defects, have not been completely modeled, an indirect method to calculate the critical stress is introduced here [37].

When a number of dislocations are accumulated in the pileup against a grain boundary due to the clearing of matrix defects, it is unlikely for the pileup dislocations to penetrate the grain boundary one by one. Once a critical stress is reached at the tip of pileup, the pileup dislocations

may avalanche into the adjoining grain in the form of two -dimensional pileup or an array. It is believed that such a rapid dynamic process should be spontaneous under the critical stress level. An idea proposed is that the stress relaxation due to an abrupt localized shear can be converted to an elastic energy release in a local volume, which is used for the propagation of a dislocation pileup [37]. It is assumed that the radiation-induced defects are completely removed within channels and thus the amount of stress relaxation is equal to the total hardening stress due to the defects. Since the shear displacement in a channel formed by glide of N_C dislocations with Burgers vector b is $N_C b$, the average shear strain in the channeled area γ_C can be given by

$$\gamma_C = \frac{N_C b}{H_C}, \tag{1}$$

where H_c is the range of stress relaxation, or the effective grain size, in which the hardening stress is relaxed. Then, the shear stress relaxed by glide of N_C dislocations is given by the product of the shear strain and shear modulus μ:

$$\tau_H = \mu\gamma_C = \frac{\mu N_C b}{H_C}. \tag{2}$$

Since the stress can not be relaxed below the yield shear stress of defect-free microstructure τ_0, the critical shear stress for channeling is approximately expressed by

$$\tau_C = \tau_0 + \frac{\mu N_C b}{H_C}. \tag{3}$$

Since a rapid channel growth was assumed in deriving this equation, the stress determined by this equation must be the critical stress for a well-developed channel only. To use equation (3), we need to evaluate the number of channeling dislocations N_c. This has been obtained from the channeled microstructures of 316 stainless steel at 0.78 dpa [3]. The largest shifts at channel intersections s_C were about 50 nm (the largest shifts should be used because the projection of the shifts appear smaller when the Burgers vector b is not on the image plane), and the size of b is 0.2526 nm for the steel. Then the number of dislocations can be calculated by the shift divided by the Burgers vector size: $N_C = s_C/b \approx 200$. Using typical material property values for 316 stainless steel, equation (3) gives about 210 MPa for the critical shear stress for channeling (or equivalent stress σ_C = 640 MPa). This level of yield stress is achieved in stainless steels by low temperature irradiation to a dose above 0.1 dpa, where channels are observed [37].

2.3.2 Twinning Stress

In fcc metals, a perfect dislocation dissociates into two Shockley partial dislocations, leaving a stacking fault between the two partials [53-54]. This separation of the Shockley partials initiates mechanical twinning at high enough stress [37,45,46]. An equilibrium separation between the two partials can be determined by a balance between the repulsive forces of the two partials and the attractive forces due to the stacking fault energy. In austenitic stainless steels, the formation of large stacking faults and twins becomes dominant when specimen is deformed at low temperatures [46,50,56] or at high strain rates [55-58]. Irradiation also significantly increases the tendency for stacking fault and twin formation [41-46]. Recently, a variety of deformation microstructures have been produced for 316 and 316LN austenitic stainless steels by changing material and testing conditions [37-46,50]). The equivalent applied stresses were calculated for those microstructures and it was attempted to find a common relationship between applied stress and deformation microstructure [45,46]. It was possible to categorize the deformation microstructures in terms of the equivalent stress range: (1) Dislocation tangles were dominant at low equivalent stresses < 400 MPa. (2) Small, isolated stacking faults smaller than about 1 μm were formed in the stress range from about 400 to 600 MPa. (3) Large stacking faults (> 1 μm) /twin bands became dominant at stresses > 600 MPa. A key conclusion was that the austenitic stainless steels will deform by forming bands of large stacking faults and twins when the stress exceeds a critical equivalent stress level of about 600 MPa by any of possible strengthening measures: irradiation, increasing strain level, and decreasing test temperature.

It is known that the perfect dislocations in fcc metals exist as dissociated partials even without external stress because of the repulsive stress between the two dissociated partials [45,54]. The distance between the two dissociated partials can be increased or decreased by external stress since the resolved shear stresses acting on the individual partial dislocations are different [54,57,59]. Copley and Kear [57] have derived an expression for the partial dislocation separation as a function of stacking fault energy and applied stress, and later Kestenbach [60] showed that the applied stress can make an average contribution of ±17% to an effective SFE in a 304 stainless steel. Goodchild et al. [59] showed that in the separation of Shockley partials the contribution due to an applied stress is of about the same magnitude as that due to SFE. In these approaches, however, the scalar treatments in formulation curtailed some degree of stress effects in the deformation associated with partial dislocations.

Byun [45] proposed a true stress-based theory for the separation of partial dislocations to explain deformation

mechanisms including the formation of large stacking faults and twins in 316 and 316LN stainless steels. The theory is introduced here to derive expressions for twinning stress and stacking fault size [37,45]. Two force balance equations for the leading and trailing partials with parallel line vectors were established by considering the Peach-Koehler force by applied stress field, the repulsive force between parallel dislocations, the attractive force due to the stacking fault energy (γ_{SF}), and the friction force [45]. It is assumed that the largest stacking faults are formed by partial glide in the x-direction on the xy-plane with dislocation line vectors in the y-direction. In this situation the shear stress τ_{zx} should be the largest or near-largest stress component. Also, the dissociation of a perfect dislocation occurs under an angular relationship between partial dislocations, θ_2-θ_1 = 60°, where θ_1 and θ_2 are the angles of the Burger's vectors of the leading and trailing partials with the dislocation line vector of the perfect dislocation, respectively. Then, the expression for separation distance of partial dislocations, *d*, is derived from the force balance equations as [45]:

$$d = \frac{\mu b_p^2 f(\theta_1, \theta_2)}{\pi(2\gamma_{SF} - \tau_{zx} b_p |\sin\theta_2 - \sin\theta_1|)}. \qquad (4)$$

where

$$f(\theta_1, \theta_2) = \cos\theta_1 \cos\theta_2 + \frac{\sin\theta_1 \sin\theta_2}{1-\nu}, \qquad (5)$$

b_p = Magnitude of the Burger's vectors of partial dislocations,
ν = Poisson's ratio.

This equation is a generalized expression for the stacking fault size as a function of stress [45]. It indicates that the separation distance increases with resolved shear stress, and the dissociation of a dislocation can increase up to infinity when the resolved stress exceeds a critical value, which becomes the twinning stress. If large stacking faults are visible on a specific {111} plane, the dissociated dislocations on the plane might be aligned properly for the maximum stress effect. The influence of external stress τ_{zx} is maximized when the Burgers vector of the perfect dislocation $\vec{b}$ coincides with the its line vector $\hat{l}$ (= $\hat{y}$), or the perfect dislocation is of pure screw type ($\hat{l} \,//\, \vec{b} \perp \tau_{zx}\,\hat{x}$), which gives simple angular relationships of the partials with the perfect dislocation: θ_1 = -30° and θ_2 = 30°.

Glide of the first Shockley partial dislocation leaves an intrinsic stacking fault behind it and needs extra stress to overcome the attractive force due to SFE [53]. It is known that the energies for intrinsic and extrinsic stacking faults and for two twin-matrix interfaces are similar [61]. Therefore, once the intrinsic stacking fault is formed by the glide of the first partial, the glide of a second partial on the next plane forms an extrinsic stacking fault behind it and erases the intrinsic stacking fault. Subsequent glide on the third and successive planes do not need additional stress to overcome the fault energy and form a twin layer [45,61,62]. Therefore, once the first partial glides, a twin layer can be formed under a high stress. In the theory discussed in Ref. [45], the twinning stress in polycrystalline material was defined by the critical stress for infinite separation of partials (with Taylor factor = 3.07 [53]):

$$\sigma_T = 3.07\tau_{crit}(d \to \infty) = 6.14\frac{\gamma_{SF}}{b_p}. \qquad (6)$$

Using equations (4) and (6), detailed calculations have been made for 316 stainless steels [45]. As indicated in equation (4), the stacking fault size, or separation distance of partials, is a function of stress. The equilibrium (zero stress) separation between partials is about 10 nm. The stress required for a 20 nm separation was calculated at about 400 MPa; which was regarded as a boundary stress between dislocation tangles and visible stacking faults [45,46]. The stresses for 30 nm and 100 nm separations were calculated at 440 MPa and 550 MPa, respectively. Also, the twinning stress was determined to be about 600 MPa from equation (6). This twinning stress is similar to the channeling stress given above, 640 MPa. Indeed, in neutron irradiated 316 stainless steels the two mechanisms compete at about 0.1 dpa or higher [3,37]. Note that a stacking fault energy of 14.2 mJ/m^2 was used for these calculations [45].

3. MACROSCOPIC STRAIN LOCALIZATION

3.1 Radiation Effects on Strain-Hardening Behaviors

The macroscopic strain localization is often called necking in tensile tests or plastic instability as a general term. The plastic instability is observed as a localized reduction of cross-sectional area that sustains load, and this occurs in any metallic materials with ductility. Irradiation usually reduces stable (or uniform) deformation capability and often erases the whole capability for uniform ductility at relatively high doses [3,18,19,36,47,49,51]. With a total loss of uniform ductility, the engineering stress-strain curve shows a decrease of engineering stress as soon as the specimen starts to yield, which is called the prompt necking at yield. Figs. 4 to 7 present some engineering stress-strain curves before and after irradiation. In the bcc A533B steel after irradiation up to 0.01 dpa, the engineering stress-strain curve consists of a few distinctive regions: elastic region, small yield drop, Lüders band, work hardening (up

to maximum stress), and plastic instability or decreasing stress. Above 0.01 dpa, however, the curves show prompt necking at yield, with vague deflection after yield drop [3]. In the hcp Zr-4, the critical stress for the prompt necking at yield is somewhere between 0.001 and 0.01 dpa. Overall flow curve behavior for the Zr-4 seems to be similar to that of A533B steel.

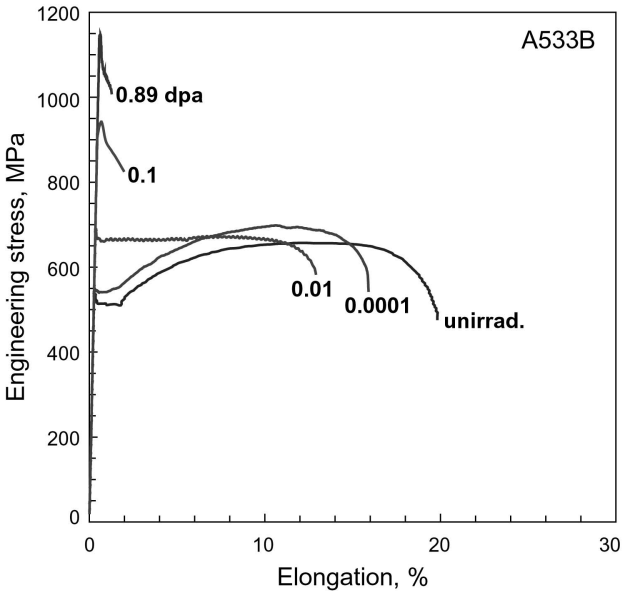

Fig. 4. Engineering Stress-strain Curves for bcc A533B Reactor Pressure Vessel Steel After Neutron Irradiation [3] Note that Prompt Necking Occurs Above 0.01 dpa. Deformed by Uniaxial Tensile Load at Room Temperature [3,36]

In plastic deformation after irradiation, most of the commercial grade pure metals and alloys behave in similar manner as the above A533B steel and Zr-4. Although the significant increase of yield stress is common for virtually all metallic materials after low temperature irradiation, some high strain-hardening rate metals such as 316 stainless steels and high purity iron show different dose dependence in the onset of necking; the prompt necking at yield is delayed to a few or a few tens of dpa. Figs. 6 and 7 are the examples. Explanation for this significant difference in the dose dependence of the onset of plastic instability has been pursued in terms of using true stress unit, instead of the engineering stress [47].

It has been repeatedly observed that the strain-hardening rate at a given strain decreases with irradiation dose. This has been explained by the clearance of radiation-induced defects by glide dislocations [1,2]. Especially the prompt necking at yield, such as those illustrated in Figs. 4 and 5, has been observed in many irradiated materials, and believed to be a direct evidence of the reduced strain-hardening capability [3]. If compared at the same stress, however, the strain-hardening portions of the flow curves after irradiation to various doses were very similar [47,49,63-66]. This indicates that the true stress-true

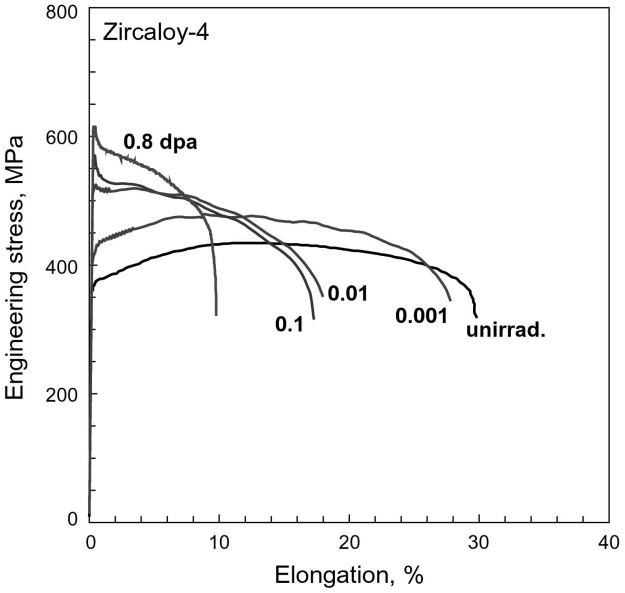

Fig. 5. Engineering Stress-strain Curves for hcp Zr-4 after Neutron Irradiation. Note that Prompt Necking Occurs Above 0.001 dpa [3]

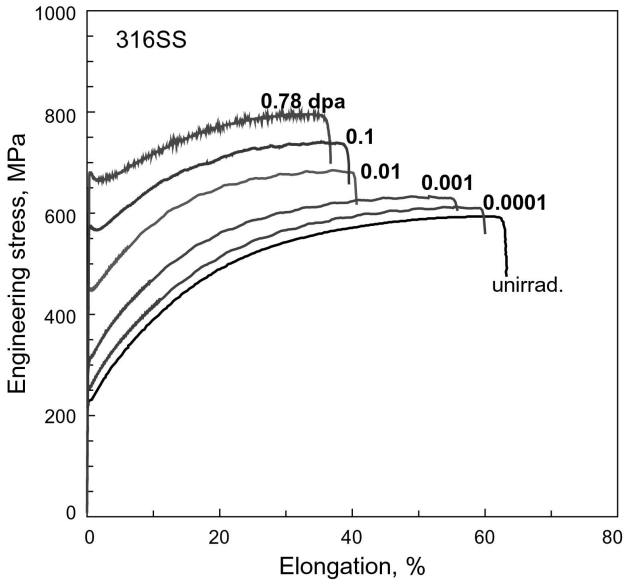

Fig. 6. Engineering Stress-strain Curves for fcc 316 Stainless Steel After Neutron Irradiation. No Prompt Necking at Yield is Found up to the Highest Dose of 0.78 dpa [3]

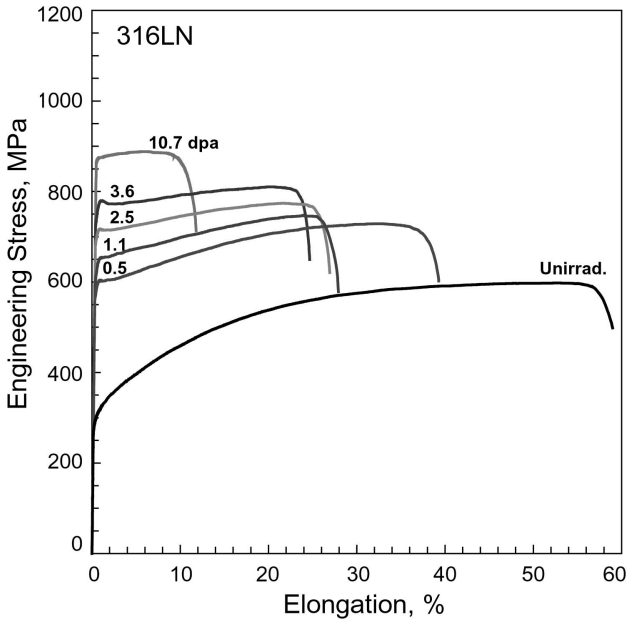

Fig. 7. Engineering Stress-strain Curves for 316LN Stainless Steel Irradiated in Spallation Condition [47]

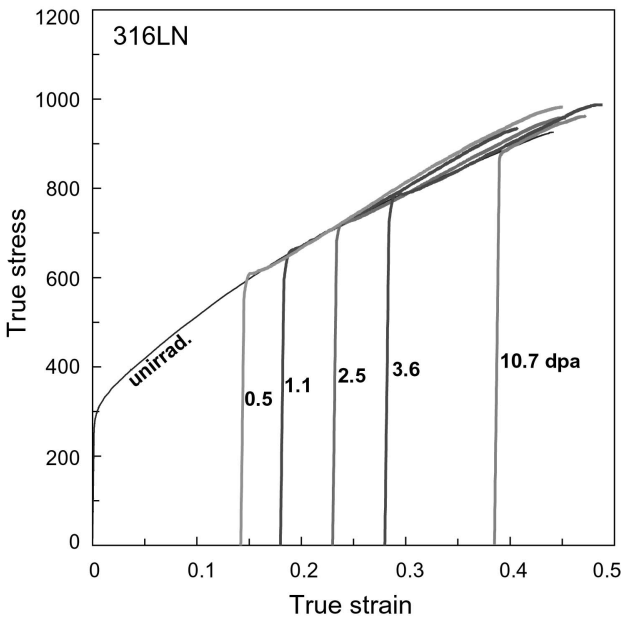

Fig. 8. True Stress-true Strain Curves for EC316LN Stainless Steel; the Curves of Irradiated Specimens are Shifted in the Positive Direction by Strains of 0.14, 0.18, 0.23, 0.28, and 0.385, Respectively, to Superimpose on the Curve of Unirradiated Material. Irradiation-induced Increases in Yield Stress Were 305, 358, 421, 485, and 587 MPa, Respectively [47]

strain curves could be superimposed on the curve for unirradiated material by shifts in the positive direction of the strain axis. Fig. 8 confirms this assertion. This leads to a conclusion that the strain-hardening behavior in neutron -irradiated iron is dose independent [65]. As an explanation for the dose independence, it was suggested that neutron irradiation has a similar effect as pre-strain on the strain-hardening rate [66], and the validity of the suggestion was tested for dozens of irradiated materials [47].

In elastic-plastic deformation, only the residual defect structure from previous deformation affects further deformation. This indicates that the strain-hardening behavior of a material is controlled by the current microstructure that determines the flow stress. Therefore, the best way to express the radiation effects on strain-hardening behavior might be a strain-hardening rate versus true stress curve, the so-called Kocks-Mecking plot [67]. The Kocks-Mecking plots for 316LN stainless steels are presented in Fig. 9. In the steel, the strain-hardening rate decreases with true stress. Excluding the transition portion of the curves near the yield point, however, all strain-hardening rates at a stress fall in a band about 500 MPa wide. Also, comparison of the curves confirms that there is no radiation-induced softening effect in strain-hardening rate. This dose independence of true stress-true strain behavior has been explained by a long-range back-stress hardening theory [24,68], which will be summarized in section 4.1.

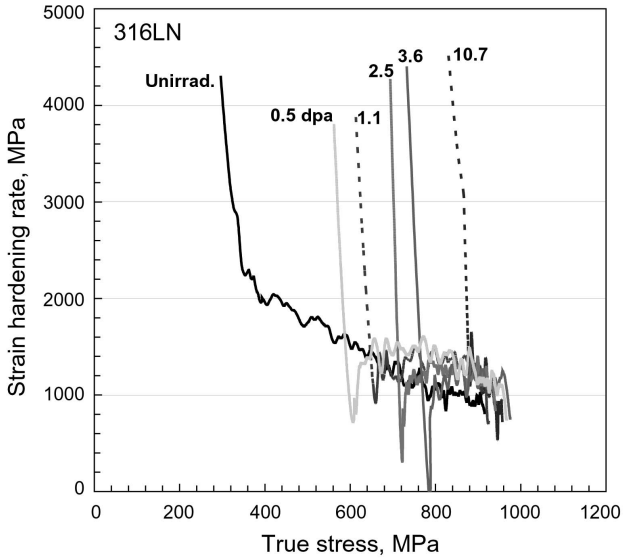

Fig. 9. Kocks-Mecking Plots (strain-hardening rate versus true stress curves) for 316LN Stainless Steel Before and After Irradiation. Except for the Elastic and Near-yield Deformation Regions, All Curves Fall Within a Narrow Band, Indicating No Significant Radiation Effect in Strain-hardening Rate [68]

3.2 Dose Dependence of True-Stress Parameters

The true stress-true strain behaviors described in the previous section indicate that the radiation influence is apparent only in yield stress. In strain hardening beyond the yield, the radiation effect is largely muted up to the onset of plastic instability. The critical true stress for the

Table 1. Data for Plastic Instability Stress [47]

Crystal Type	Materials	Dose Range, dpa	PIS (at 0 dpa), MPa	PIS (average in the dose range 0 - D_C), MPa	D_C, dpa
bcc	A533B-a	0 - 0.89	715	732	0.02
bcc	A533B-b	0 - 1.2	665	680	0.015
bcc	A533B-c	0 - 1.28	670	678	0.02
bcc	3Cr-3WV	0 - 1.2	707	705	0.025
bcc	9Cr-1MoVNb	0 - 1.2	748	752	0.034
bcc	9Cr-2VWTa	0 - 1.2	764	783	0.054
bcc	9Cr-2WV	0 - 1.2	753	768	0.054
bcc	9Cr-2VWTa	0 - 10.2	773	802	0.12
bcc	Mod. 9Cr-1Mo	0 - 10.2	745	767	0.09
bcc	Fe-a	0 - 0.79	304	306	0.2
bcc	Fe-b	0 - 1.07	291	291	6
bcc	Nb	0 - 0.37	368	368	0.007
bcc	V	0 - 0.69	397	393	0.0017
fcc	316-a	0 - 0.78	901	975	27
fcc	316-b	0 - 1.2	925	941	35
fcc	316LN	0 - 1.2	948	935	40
fcc	EC316LN	0 - 10.7	883	948	22
fcc	HTUPS316	0 - 10.7	709	785	5
fcc	AL6XN	0 - 10.7	961	996	17
fcc	Cu	0 - 0.92	300	303	0.12
fcc	Ni	0 - 0.6	541	530	0.15
hcp	Zr-4-a	0 - 0.8	512	524	0.009
hcp	Zr-4-b	0 - 24.6	500	500	0.004
hcp	Zr	0 - 0.63	159	173	0.09

D_C = dose to plastic instability at yield.

onset of necking was defined as the plastic instability stress (PIS), and it can be calculated from the ultimate load and uniform strain measurements [47,49]. The PIS parameter was established as a common stress criterion for the onset of plastic instability for both unirradiated and irradiated materials since the dose independence of the PIS was well confirmed in the extended studies [47,48]. The PIS values for unirradiated and irradiated materials are listed in Table 1.

Although the true stress-true strain curve after the onset of necking is not known, it is possible to estimate the true fracture stress based on a linear strain hardening model for necking deformation [37,51]. The comparison of strain-hardening rate during necking (HRN) with PIS values revealed that the magnitude and temperature dependence of HRN were approximately the same as those of the PIS above room temperature, where no martensitic transformation occurred [50]. This confirms that the strain-hardening rate is positive during necking although the engineering stress decreases with elongation. This should be valid as long as there is a diffuse neck, which occurs usually in ductile metals before a final failure by localized shear (banding) or cleavage initiation. The finding that the strain-hardening rate remains nearly unchanged at plastic instability stress during necking leads to the use of linear true stress-true strain curves for necking deformation [37].

With constant strain-hardening rates during necking, a true stress-true strain curve during necking ($\varepsilon_U \le \varepsilon \le \varepsilon_F$) can be expressed by a linear equation [37,51]:

$$\sigma(\varepsilon) = \max(YS, PIS) + PIS(\varepsilon - \varepsilon_U), \quad (7)$$

where ε_U and ε_F are the true uniform strain and the fracture strain, respectively. Then, the true fracture stress FS can be calculated by replacing ε with ε_F in equation (7).

$$FS = \max(YS, PIS) + PIS(\varepsilon_F - \varepsilon_U), \quad (8)$$

or from the engineering fracture stress (EFS) using the volume constant condition:

$$FS = EFS \times \exp(\varepsilon_F). \quad (9)$$

The solution for ε_F and FS can be obtained by iterative calculations using equations (8) and (9) and engineering tensile data.

A deformation mode map can be formed by expressing macroscopic deformation modes, elastic, uniform plastic, and necking deformations, in true stress versus dose space. In such a map the true stress parameters such as yield stress, plastic instability stress, and true fracture stress are used as the boundaries between the deformation modes. Figures 10 and 11 present the dose dependencies of true stresses (or macroscopic deformation maps) for pure vanadium (bcc) and 316 stainless steel (fcc) [51]. In the pure vanadium after low temperature neutron irradiation up to 0.69 dpa, the true fracture stress is nearly independent of dose with small scattering. Moreover, the plastic instability stress is almost constant with smaller scatter [47,51]. Only the yield stress shows significant dose dependence. Also, it was noticed in the Fig. 10 that the fracture stress dropped to the yield stress value at 0.68 dpa, indicating that the specimen was totally embrittled during irradiation. Such evidences for radiation embrittlement were often displayed in some relatively low-ductility materials. In 9Cr-1MoVNb and 9Cr-2WVTa ferritic-martensitic steels, for example, the true fracture stress was roughly constant over a dose range of 0 – 1 dpa, while it decreased with dose after about 1 dpa until it experienced a total embrittlement at ~ 10 dpa [51].

Figure 10 depicts the regions for macroscopic deformation modes such as the elastic deformation, uniform plastic deformation, and unstable (necking) deformation; the regions of these modes are defined by the true stress parameters. Comparing the sizes of the regions for deformation modes, the mode maps for bcc metals are characterized by a relatively large plastic instability region and a narrow uniform deformation region, which should be due to large necking ductility and low strain-hardening rate, respectively.

Figure 11 presents the macroscopic deformation mode map for 316 austenitic stainless steel. Again, the plastic instability stress and fracture stress are nearly independent of dose. In this fcc deformation mode map, the uniform deformation region is relatively large when compared to the plastic instability region. This large uniform deformation region indicates more delayed necking in the 316 stainless steel. The yield stress of 316 stainless steel will not reach the plastic instability stress until about 30 dpa, while in the bcc vanadium the yield stress reaches the plastic instability stress between 0.001 and 0.01 dpa [36,51]. These differences between bcc and fcc metals agree with the fact that the strain-hardening rate in fcc metals are generally higher than those in bcc metals, especially in high strain region. The dose dependence of true stress parameters for hcp metals was not significantly different from those for bcc metals [51].

Thus far, most of studies on strain-hardening behavior have been focused on stable or uniform deformation. In the explanation of fracture behavior, however, the unstable deformation during necking might be as important as the uniform deformation since mechanical property like fracture toughness is directly related to the fracture strain (and stress), and significant true necking strains are often measured from the irradiated specimens which experience necking at yield. In fact, the significance of unstable

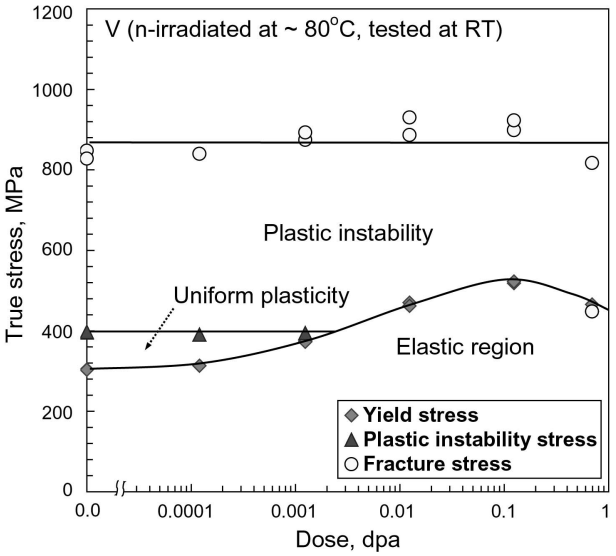

Fig. 10. Dose Dependence of True Stress Parameters in Pure Vanadium After Low Temperature Neutron Irradiation

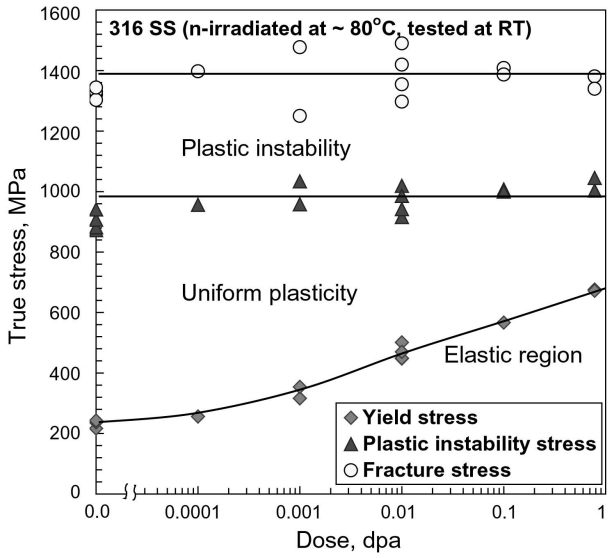

Fig. 11. Dose Dependence of True Stress Parameters in 316 Stainless Steel After Low Temperature Neutron Irradiation [51]

deformation is presented in the macroscopic deformation mode maps for bcc and hcp metals, Figs. 10, as an example, where the unstable deformation region is much larger than the uniform deformation region [51]. Above the critical dose for prompt necking at yield, only unstable deformation exists and controls the performance of the material. Until the material is totally embrittled either by a decrease of fracture stress, or by an increase of yield stress, the unstable deformation plays a major role in the determination of fracture toughness, particularly in the bcc and hcp alloys where the unstable deformation region is larger compared to the uniform deformation region. Since the final rapid fracture is the end event of strain hardening, the radiation effect on strain-hardening behavior should be emphasized in describing any fracture-related properties after irradiation. The final conclusion drawn from the invariance of strain-hardening behavior is that the fracture stress should be nearly independent of irradiation dose if no embrittlement mechanism exists [51].

4. GENERALIZATION OF STRAIN LOCALIZATION

Descriptions in the previous sections indicate that the true strain-hardening rate at a given true stress is not significantly affected by the microscopic strain localization [47,49]. Although the detailed mechanism of channel formation is largely unknown, a number of studies have confirmed that defect clusters are cleared by gliding dislocations within channels [4-13]. A significant drop of local shear stress in the channel may occur because of this clearance in the early stage of channel formation. In twinning, a significantly reduced stress is necessary after the glide of the first partial forms stacking fault. If the macroscopic strain-hardening rate remains unchanged with strain localization, however, the softening effect from the defect clearance or stacking fault formation is a local, temporary event and the local stress level should return quickly to a level as high as those in adjacent regions [24,47]. This indicates that certain mechanism in the localized deformation compensates the softening effect in the bands.

Byun and Farrell [47] suggested two possible reasons for the dose independence of strain-hardening behavior: (1) Similar true strain-hardening behaviors can be produced by the channel deformation in irradiated materials and by the uniform deformation in unirradiated materials. (2) Deformations in irradiated materials and in heavily-deformed unirradiated materials are both equally localized. If the first suggestion is correct, the strain-hardening rate due to long-range back stresses in the channels and twins in irradiated metals should be as high as that in the region of uniform deformation in unirradiated metals. Also, to justify the second suggestion, we have to observe microscopic strain localization in the dislocation tangle dominant microstructures.

4.1 Long-Range Stress in Localized Deformation

A theoretical model was proposed to elucidate the importance of the long-range back stress in strain hardening

during strain localization [24]. In the modeling the long-range back stress was formulated as a function of the number of residual pileup dislocations at a grain boundary and the number of localized bands formed in a grain. Two different features were taken into account to discern the channeling and twinning mechanisms [24,68]. First, the sizes of the Burgers vectors are different for perfect and partial dislocations. Second, the stacking faults always exist with twins, and the fault energy (γ_{SF}) acts as a resistance force to the glide. In the theory summarized below, channeling is described first and the two features were incorporated to convert the channeling model to the twinning model.

This channeling model involves a well-developed defect-free channel only, in which most of shear plasticity has already propagated into adjoining grains leaving white bands in the edge-on TEM micrographs [24]. Since the channel displacement, $N_C b$, cannot be completely transferred to the adjoining grain by glide to the same direction unless the orientations of the two grains are perfectly identical, some amount of the displacement must remain at the grain boundary. Considering that dislocations are scarcely observed at an intersection between the grain boundary and the well -developed channel [1-4], only a small portion of total displacement is believed to remain in the form of a small dislocation pileup. Since the back stress from a pileup of a few hundred dislocations can easily exceed the flow stress level of the material and stop further slip, clear channels may be developed only in the grains having similarly-oriented adjoining grains to which the channels can easily propagate. A highly simplified graphical model for the channeled grain was used to derive an equation for total back stress; the grains include multiple channels and each channel retains a few residual dislocations at the grain boundary [24]. If a small pileup of N_R residual edge dislocations exist in the ith channel at a grain and dislocations are being generated at a source, the back stress exerted to the source can be calculated from the stress fields from the residual dislocations piled up at the grain boundary [53-55]. Assuming there are N_G channels in the grain, the shear component of total back stress at a dislocation source is calculated by the summation of back-stress components in individual channels:

$$\tau_B = \frac{\mu N_R b}{2\pi(1-\nu)} \sum_{i=1}^{N_G} \frac{L(L^2 - h_i^{\,2})}{(L^2 + h_i^{\,2})^2} . \qquad (10)$$

where L and h_i are defined as the effective grain size and vertical distance between the source and the residual pileup, respectively.

Again, the present twinning model treats the well-developed twins only, such as those seen in Figs. 3(c) and 3(d). No interaction between twins or between twins and channels was considered; if any, smaller twins might be formed and the strain-hardening behavior becomes similar to that by dislocation tangles or often cell structures. It is known that deformation twins are formed by successive glide of partial dislocations of pure screw component [45,60-62]. As stated earlier, glide of the first Shockley partial dislocation leaves an intrinsic stacking fault behind it and only the first partial needs an extra stress to overcome the attractive force due to the stacking fault energy ($= \gamma_{SF}/b_p$). Subsequent glides on the successive planes do not need additional stress to overcome the fault energy and form a twin layer. Since radiation-induced defects are not completely removed by twinning [42], the softening effect by glide of the first partial may play a major role in the forming and thickening of a twin by inducing subsequent glide of partial dislocations.

To consider these features of twinning, the relationship developed for channeling, equation (1), should be modified: the magnitude of Burgers vector for a partial dislocation, b_p, is used and the position function is for a pure screw dislocation:

$$\tau_B = \frac{\mu N_R b_p}{2} \sum_{i=1}^{N_G} \frac{L}{L^2 + h_i^{\,2}} . \qquad (11)$$

To evaluate above equations (10) and (11), the number of residual dislocations N_R and the number of channels in a grain N_G need to be estimated. Detailed procedures for calculating these parameters are described elsewhere [24,68]. Since the long-range stress hardening is caused by the dislocations which pile up at a grain boundary, the number of the pileup dislocations is a key parameter in the calculation. Table 2, for example, lists the number of residual dislocations, along with other dislocation number data. The results confirm that hundreds of dislocation glides are necessary to form a channel or a twin; the number of gliding dislocations per channel, N_C, are in the range 300 – 500. It turned out, however, that a few residual dislocations at each channel-grain boundary intercept could account for the strain-hardening rates as high as those for the uniform deformation by dislocation tangling [24,68]. The total number of residual dislocations will keep increasing as more channels are formed in a given volume, and therefore the density of residual dislocation (last column in the table) increased with strain. Mechanical twinning formed more bands, which was necessary to accommodate macroscopic strain with the smaller Burgers vector of partial dislocations.

It was shown that the strain-hardening behavior predicted by the long-range back stress model resembled the empirical strain-hardening behaviors which result from both localized and non-localized deformations [24]. The result is provided in Fig. 12, where the PIS values predicted for channeling was well comparable to the tensile test data. These results,

Table 2. Dislocation Numbers at PIS Calculated for the Highest Dose Cases [68]

Mater.	Deformation Mechanism	Dose, dpa (radiation)	Stress, MPa (predicted PIS)	Strain	N_C	N_G	N_R	$N_G \times N_R / L$ (residual dislocations/μm)
316	Channel	0.78 (n)	1010	0.29	307	117	2.3	27
316	Twin	0.78 (n)	900	0.31	493	132	3.1	41
316LN	Channel	10.7 (n+p)	950	0.09	291	24	2.3	6
316LN	Twin	10.7 (n+p)	940	0.09	493	36	3.1	11

Note : n-neutron; n+p-neutron and proton,
N_C = the # of glide dislocations per channel,
N_G = the # of channels per grain,
N_R = the # of residual dislocations per channel, and
$N_G \times N_R / L$ = the density of residual dislocation (per unit length of grain boundary)

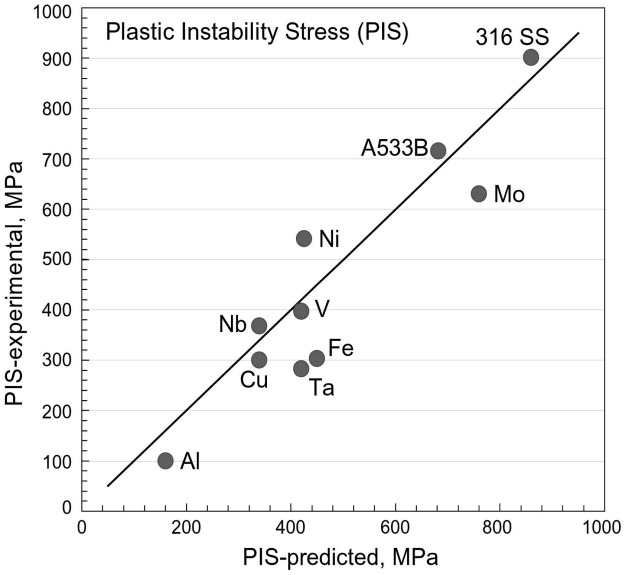

Fig. 12. Comparison of Predicted Plastic Instability Stresses with Experimental Data [24]

therefore, indicates that at least the first term (1) in above suggestions is valid; the strain localization is not accompanied by significant change in macroscopic mechanical property or strain-hardening behavior, except for the increase of yield stress, which often comes with a yield drop.

4.2 Generalization of Strain Localization

There is also supporting evidence for the second suggestion above: channels can be formed in unirradiated materials after heavy pre-deformation. Such channel deformation has been reported for copper [69], molybdenum [70-71], and aluminum [72]. In these results, macroscopic strain-hardening rates were positive, although localized (channeled) deformation was observed. This suggests that the dislocation channeling is a common phenomenon for any high stress deformations. Whether the material is irradiated or not, a possible driving force to initiate microscopic strain localization could be a local softening effect due to the dislocation annihilation (or dynamic recovery), which is analogous to the defect clearing process in irradiated materials. It is also proposed that the localized deformation will occur in any highly strengthened material if dislocation glide can induce a local softening or reduced hardening rate. It is seen most readily in transmission electron microscopy examination of irradiated materials because the radiation damage microstructure provides a sharp contrast backdrop to the cleaned channels, while it should be difficult to detect in pre-strained materials because of lack of contrast.

Another good example for the generalization of strain localization is the twins formed after heavy deformation in austenitic stainless steels. As mentioned in sections 2 and 4, a softening effect is induced by formation of stacking fault by glide of the first partial [45]. Twinning also becomes dominant in the high stress condition imposed by deformation at cryogenic temperatures below ~100 ℃ [50].

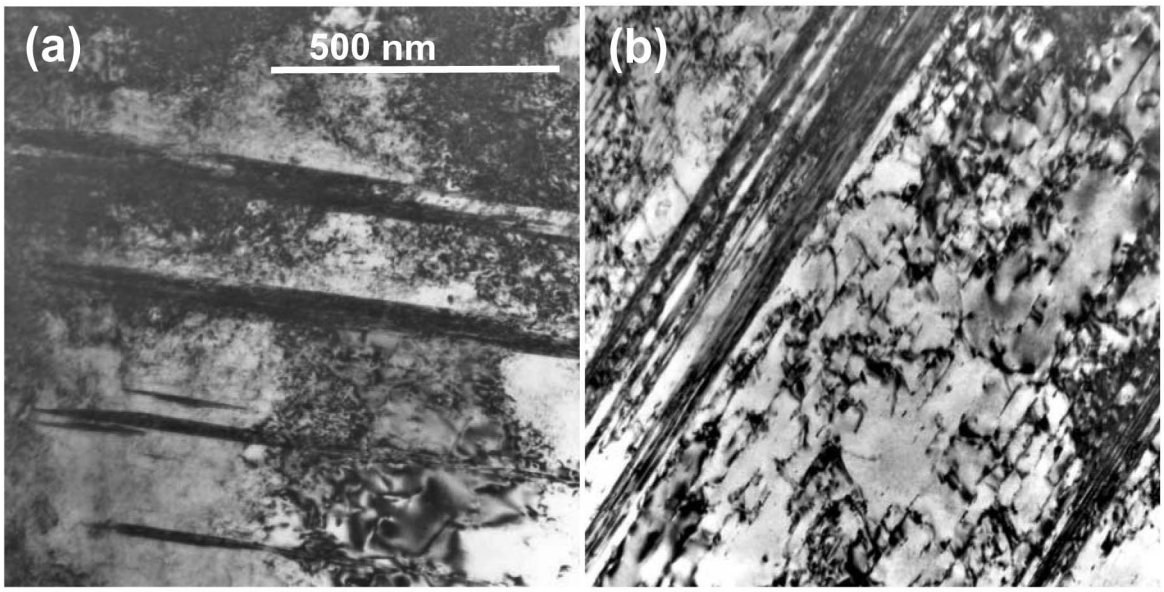

Fig. 13. Twins (dark bands) Formed in Heavily-deformed 316 Stainless Steel [3,37]: Twins Formed on the Top of Dense Dislocation Tangles (a) at 0 dpa, 57% Strain and (b) at 0.001 dpa, 55% Strain

Examples for the twins not involving irradiation are shown in Figs. 13(a) and 13(b), where thick twins are clearly seen in heavily deformed specimens with heavy dislocation tangles as background [50,68].

Although the evidences reported may not be sufficient to confirm the strain localization as a general high stress phenomenon, the existing results provide important evidences for the thought that the localized deformation occurs more easily at higher stresses, usually exacerbated by a lowered strain-hardening rate.

5. SUMMARY

Both the macroscopic and microscopic strain localization phenomena in irradiated materials are reviewed and characterized in this paper, emphasizing the latest findings at ORNL. A summary is given as below:

[1] Microscopic localization mechanisms observed in irradiated metals are the dislocation channeling and defor-mation twinning. In channeling ordinary dislocations glide along the limited slip planes within a band, removing or cutting through small barriers in their paths. This defect-clearing interaction creates an easy path for subsequent dislocation glide and a narrow channel is developed. In some high stacking energy bcc materials such as vanadium and molybdenum, curved and widening channels can be formed depending on dose and stress state. In low SFE fcc materials, the deformation twins can be formed after irradiation by glide of Shockley partial dislocations on successive {111} planes. In such a twin, shear strain is ~70% and the number density of defects is reduced by glide of partial dislocations. In both mechanisms dislocation glides are evenly distributed and well confined in the narrow bands usually a fraction of a micron wide.

[2] The effect of irradiation on the true stress-true stain curve is increase of yield stress and loss of uniform ductility; however, after the yield point the strain-hardening behavior is not evidently affected by irradiation at the same true stress level. This agrees with the other important findings that the plastic instability stress and true fracture stress are nearly independent of dose if there is no radiation-induced phase change or embrittlement.

[3] No evident relationship between the microscopic and macroscopic strain localizations is found. This is explained by long-range back-stress hardening in both channeling and twinning deformations; dominant strain-hardening mechanism changes from the dislocation tangling (or others) in uniform deformation to the long-range stress hardening in localized deformation.

[4] The strain localization has been observed in the high stress deformations such as high speed deformation, low temperature deformation, and deformation after irradiation or heavy pre-straining. It is believed that additional research efforts can confirm the strain localization as a general high stress phenomenon.

ACKNOWLEDGEMENTS

This research was sponsored by U.S. Department of Energy, Office of Fusion Energy Sciences, under Contract DE-AC05-00OR22725 with UT-Battelle, LLC. The author would like to express special thanks to Drs. J.T. Busby and M.M. Li for their technical reviews and thoughtful comments.

REFERENCES

[1] M.S. Wechsler, "Dislocation Channeling in Irradiated and Quenched Metals," *The Inhomogeneity of Plastic Deformation, American Society for Metals*, pp.19-54 (1971), Metals Park, Ohio.
[2] A. Luft, "Microstructural Processes of Plastic Instabilities in Strengthened Metals," *Progress in Materials Science*, **35**, 97 (1991).
[3] K. Farrell, T.S. Byun, N. Hashimoto, "Deformation Mode Maps for Tensile Deformation of Neutron-irradiated Structural Alloys," *J. of Nucl. Mater*., **335**, 471 (2004).
[4] F.A. Smidt, Jr., "Dislocation Channeling in Irradiated Metals," NRL-7078, Naval Research Laboratory (1970).
[5] M.J. Makin and F.J. Minter, "Irradiation Hardening in Cooper and Nickel," Acta Metall., **8**, 691 (1960).
[6] A.G. Greenfield, A.G.F. Wilsdorf, "Effect of Neutron Irradiation on the Plastic Deformation of Copper Single Crystals," *J. Appl. Phys*., **32**, 827 (1961).
[7] M.J. Makin and J.V. Sharp, "A Model of Lattice Hardening in Irradiated Copper Crystals with the External Characteristics of Source Hardening," *Physics Stat. Sol*., **9**, 109 (1965).
[8] J.V. Sharp, "Deformation of Neutron Irradiated Cooper Single Crystals," *Phil. Mag*., **16**, 77 (1967).
[9] A.J.E. Foreman and J.V. Sharp, "A Mechanism for Sweeping -up of Loops by Glide Dislocations during Deformation," Phil. Mag., **19**, 931 (1969).
[10] R.P. Tucker, M.S. Wechsler and S.M. Ohr, "Dislocation Channeling in Neutron-Irradiation Niobium," *J. Appl. Phys*., **40**, 400 (1969).
[11] J.V. Sharp, "Deformation of Neutron Irradiated Copper Alloys," *Acta Metall*., **22**, 449 (1974).
[12] Y. Huang, E. Pink, and R.J. Arsenault, "Radiation Effects on the Yield Stress and Dislocation Channeling in Neutron Irradiated Molybdenum," Metall. Trans., **5**, 271 (1974).
[13] T. Onchi, H. Kayano and Y. Higashiguchi, "The Inhomogeneous Deformation Behaviour of Neutron Irradiated Zircaloy - 2," J. Nucl. Mater, **88**, 226 (1980).
[14] J. Gazda, M. Meshii, H. M. Chung, "Microstructure of V-4Cr-4Ti Alloy after Low-Temperature Irradiation by Ions and Neutrons, J. of Nucl. Mater., **258-263**, 1473 (1998).
[15] S.A. Maloy, M.R. James, W.R. Johnson, T.S. Byun, K. Farrell, M.B. Toloczko, "Comparison of Fission Neutron and Proton/Spallation Neutron Irradiation Effects on the Tensile Behavior of Type 316 and 304 Stainless Steel," *J. of Nucl. Mater*., **318**, 283 (2003).
[16] G.S. Was, J.T. Busby, "Role of Irradiated Microstructure and Microchemistry in Irradiation-Assisted Stress Corrosion Cracking," *Phil. Mag*., **85**, 443 (2005).
[17] B.N. Singh, A.J.E. Foreman, H. Trinkaus, "Radiation Hardening Revisited: Role of Interacascade Clustering," *J. of Nucl. Mater*. **249**, 103 (1997).
[18] B.N. Singh, A. Horsewell, P. Toft, "Effects of Neutron Irradiation on Microstructure and Mechanical Properties of Pure Iron," *J. Nucl. Mater*., **271&272**, 97 (1999).
[19] M. Victoria, N. Baluc, C. Bailat, Y. Dai, M.I. Luppo, R. Schäublin, B.N. Singh, "The Microstructure and Associated Tensile Properties of Irradiated fcc and bcc Metals," *J. Nucl. Mater*. **276**, 114 (2000).
[20] C. Bailat, F. Gröschel, M. Victoria, "Deformation Modes of Proton and Neutron Irradiated Stainless Steels," *J. Nucl. Mater*. **276**, 283 (2000).
[21] T.S. Byun, K. Farrell, E.H. Lee, J.D. Hunn, L.K. Mansur, "Strain Hardening and Plastic Instability Properties of Austenitic Stainless Steel after Proton and Neutron Irradiation," *J. of Nucl. Mater*., **298**, 269 (2001).
[22] T.A. Khraishi, H.M. Zbib, T. D. de la Rubia, and M. Victoria, "Localized Deformation and Hardening in Irradiated Metals: Three-Dimensional Discrete Dislocation Dynamics Simulations," *Metall. & Mater. Trans*. **33B**, 285 (2002).
[23] Hashimoto, T. S. Byun, and K. Farrell, "Microstructural Analysis of Deformation in Neutron-Irradiated fcc Materials," *J. of Nucl. Mater*., **351**, 295 (2006).
[24] T.S. Byun, N. Hashimoto, "Strain Hardening and Long Range Internal Stress in the Localized Deformation of Irradiated Polycrystalline Metals," *J. of Nucl. Mater*., **354**, 123 (2006).
[25] L.K. Mansur, A.F. Rowcliffe, R.K. Nanstad, S.J. Zinkle, W.R. Corwin, R.E. Stoller, "Materials Needs for Fusion, Generation IV Fission Reactors and Spallation Neutron Sources - Similarities and Differences," *J. of Nucl. Mater*., **329**, 166 (2004).
[26] S.G. Song, J.I. Cole and S.M. Bruemmer, "Formation of Partial Dislocations During Intersection of Glide Dislocations with Frank Loops in f.c.c Lattices," Acta Mater., **45**, 501 (1997).
[27] E. Johnson and P.B. Hirsch, "*In Situ* Straining in the HVEM of Neutron-Irradiated Cooper Crystals," Phil. Mag. A, **43**, 157 (1981).
[28] M. Suzuki, A. Fujimura, A. Sato, J. Nagakawa, N. Yamamoto and H. Shiraishi, "*In Situ* Deformation of Proton-Irradiated Molybdenum in a High-Voltage Electron Microscope," Phil. Mag. A, **64**, 395 (1991).
[29] M. Suzuki, A. Sato, T. Mori, J. Nagakawa, N. Yamamoto, H. Shiraishi, "*In Situ* Deformation and Unfaulting of Interstitial Loops in Proton-Irradiated Steels," *Phil. Mag. A*, **65**, 1309 (1992).
[30] Y. Matsukawa, Y.N. Osetsky, R.E. Stoller, S.J. Zinkle, "Destruction Processes of Large Stacking Fault Tetrahedra Induced by Direct Interaction with Gliding Dislocations," *J. of Nucl. Mater*, **351**, 285 (2006).
[31] J.S. Robach, I.M. Robertson, B.D. Wirth and A. Arsenlis, "*In-Situ* Transmission Electron Microscopy Observation and Molecular Dynamics Simulations of Dislocation-Dffect Interactions in Ion-Irradiated Copper," *Phil. Mag*., **83**, 955 (2003).
[32] T.D. de la Rubia, H.M. Zbib, T.A. Khraishi, B.D. Wirth,

M. Victoria and M.J. Caturla, "Multiscale Modeling Plastic Flow Localization in Irradiated Materials," *Nature*, **406**, 871 (2000).
[33] M. Hiratani, H.M. Zbib, and B.D. Wirth, "Interaction of Glissile Dislocations with Perfect and Truncated Stacking-Fault Tetrahedra in Irradiated Metals," *Phil. Mag*. A, **82**, 2709 (2002).
[34] D.J. Bacon, Y.N. Osetsky, Z. Rong, "Computer Simulation of Reactions between an Edge Dislocation and Glissile Self-Interstitial Clusters in Iron," *Phil. Mag*., **86**, 3921 (2006).
[35] Y.N. Osetsky, D. Rodney, D.J. Bacon, "Atomic-Scale Study of Dislocation-Stacking Fault Tetrahedron Interactions. Part I: Mechanisms," *Phil. Mag*., **86**, 2295 (2006).
[36] N. Hashimoto, T.S. Byun, K. Farrell, S.J. Zinkle, "Deformation Microstructure of Neutron-Irradiated Pure Polycrystalline Vanadium", *J. of Nucl. Mater*., **336**, 225 (2005).
[37] T.S. Byun, N. Hashimoto, and K. Farrell, "Deformation Mode Map of Irradiated 316 Stainless Steel in True Stress-Dose Space", *J. of Nucl. Mater*., **351**, 303 (2005).
[38] T.S. Byun, N. Hashimoto, K. Farrell, E.H. Lee, "Characteristics of Microscopic Strain Localization in Irradiated 316 Stainless Steels and Pure Vanadium," *J. of Nucl. Mater*., **349**, 251 (2006).
[39] Y. Dai, X. Jia, J.C. Chen, W.F. Sommer, M. Victoria, G.S. Bauer, "Microstructure of Both As-Irradiated and Deformed 304 Stainless Steel Irradiated with 800 MeV Protons," *J. Nucl. Mater*. **296**,174 (2001).
[40] C. Bailat, A. Almazouzi, N. Baluc, R. Schaublin, F. Groschel, M. Victoria, "The Effects of Irradiation and Testing Temperature on Tensile Behavior of Stainless Steel," *J. Nucl. Mater*. **283,** 446 (2000).
[41] E. H. Lee, J. D. Hunn, T. S. Byun, and L. K. Mansur, "Effects of Helium on Radiation-Induced Defect Microstructure in Austenitic Stainless Steel," *J. of Nucl. Mater*., **280**, 18 (2000).
[42] E.H. Lee, T.S. Byun, J.D. Hunn, M.H. Yoo, K. Farrell and L.K. Mansur, "On the Origin of Deformation Microstructures in Austenitic Stainless Steel: Part I- Microstructures," *Acta Mater*., **49**, 3269 (2001).
[43] E.H. Lee, M.H. Yoo, T.S. Byun, J.D. Hunn, K. Farrell and L.K. Mansur, "On the Origin of Deformation Microstructures in Austenitic Stainless Steel: Part II-Mechanisms," *Acta Mater*., **49**, 3277 (2001).
[44] T.S. Byun, E.H. Lee, J.D. Hunn, K. Farrell, L.K. Mansur, "Characterization of Plastic Deformation in a Disk Bend Method," *J. of Nucl. Mater*., **294**, 256 (2001).
[45] T.S. Byun, "On the Stress Dependence of Partial Dislocation Separation and Deformation Microstructure in Austenitic Stainless Steels," *Acta Mater*., **51**, 3063 (2003).
[46] T.S. Byun, E.H. Lee, and J.D. Hunn, "Plastic Deformation in 316LN Stainless Steel – Characterization of Deformation Microstructures," *J. of Nucl. Mater*., **321**, 29 (2003).
[47] T.S. Byun and K. Farrell, "Plastic Instability in Polycrystalline Metals after Low Temperature Irradiation," *Acta Mater*., **52**, 1597 (2004).
[48] T.S. Byun and K. Farrell, "Irradiation Hardening Behavior of Polycrystalline Metals after Low Temperature Irradiation," *J. of Nucl. Mater*., **326**, 86 (2004).
[49] T. S. Byun, K. Farrell, and N. Hashimoto, "Plastic Instability Behavior of bcc and hcp Metals after Low Temperature Neutron Irradiation," *J. of Nucl. Mater*., **329-333**, 998 (2004).
[50] T. S. Byun, N. Hashimoto, K. Farrell, "Temperature Dependence of Strain Hardening and Plastic Instability Behaviors in Austenitic Stainless Steels," *Acta Mater*., **52**, 3889 (2004).
[51] T.S. Byun, "Dose Dependence of True Stress Parameters in Irradiated bcc, fcc, and hcp Metals." *Wechsler Symposium on Radiation Effects, Deformation and Phase Transformation in Metals and Ceramics in 2006 TMS Annual Meeting*, San Antonio, TX, USA, March 12-16, 2006. (To be published in J. of Nucl. Mater.)
[52] A.H. Cottrell, "Vacancies and Other Point Defects in Metals and Alloys," *The Institute of Metals*, London (1958).
[53] R.W. Hertzberg, *Deformation and Fracture Mechanics of Engineering Materials*, 3rd Ed., John Wiley and Sons, Inc., pp.67-80 (1989), New York.
[54] J.P. Hirth, J. Lothe, *Theory of dislocations*, McGraw-Hill Book Co, (1968), New York.
[55] M.A. Meyers, K.K. Chawla, *Mechanical behavior of materials*, Prentice-Hall, Inc., (1998), Upper Saddle River, NJ.
[56] J.W. Christian, S. Mahajan, "Deformation Twinning," *Prog. In Mater. Sci*., **39**, 1 (1995).
[57] S.M. Copley, B.H. Kear, "The Dependence of the Width of a Dissociated Dislocation on Dislocation Velocity," Acta Metall., **16**, 227 (1968).
[58] B.H. Sencer, S.A. Maloy, G.T. Gray III, "The Influence of Explosive-Driven Shock Prestraing at 35 GPa and High Deformation on the Structur/Property Behavior of 316L Austenitic Stainless Steel," *Metall. Mater. Trans*., **36A**, 1825, (2005).
[59] D. Goodchild, W.T. Roberts, D.V. Wilson, "Plastic Deformation and Phase Transformation in Textured Austenitic Stainless Steel," *Acta Metall*, **18**, 1137 (1970).
[60] H.J. Kestenbach, "The Effect of Applied Stress on Partial Dislocation Separation and Dislocation Structure in Austenitic Stainless Steel," *Phil. Mag*. **36**, 1509 (1977).
[61] Z. Jin, T.R. Bieler, "A Numerical Force and Stress Analysis on a Thin Twin Layer in TiAl," *Phil. Mag. A*, **72**, 1201 (1995).
[62] Z. Jin, T.R. Bieler, "An In-Situ Observation of Mechanical Twin Nucleation and Propagation in TiAl," *Phil. Mag. A*, **71**, 925 (1995).
[63] S.M. Ohr, "Work Hardening Characteristics of Neutron Irradiated Iron," Scripta Metall., **2**, 213 (1968).
[64] E.V. van Osch, M.I. de Vries, "Irradiation Hardening of V-4Cr-4Ti," J. Nucl. Mater., **272-272**, 162 (1999).
[65] R.J. DiMelfi, D.E. Alexander, L.E. Rehn, "Post-Yield Strain Hardening Behavior as a Clue to Understanding Irradiation Hardening," J. Nucl. Mater., **252**, 171 (1998).
[66] I.L. Mogford, D. Hull, "Effect of Temperature and Neutron Irradiation on Yield and Work Hardening in Iron," *J. Iron Steel. Inst*., **201**, 55 (1963).
[67] U.F. Kocks, H. Mecking, "Physics and Phenomenology of Strain Hardening: the FCC Case," Progress in Materials Science, **48**, 171, (2003).
[68] T.S. Byun, N. Hashimoto, "Strain Hardening during Mechanical Twinning and Dislocation Channeling in Irradiated 316 Stainless Steels," *23rd ASTM Symposium on Effects of Radiation on Materials*, San Jose, CA, June 13-15, 2006.
[69] Z.S. Basinski and P.J. Jackson, "The Effect of Extraneous Deformation on Strain Hardening in Cu Single Crystals," *Appl. Phys. Lett*., **6**, 148 (1965).
[70] C. Ritschel, A. Luft, and D. Schulze, "On the Change of Dislocation Structure during Post-Deformation of Cold Worked Molybdenum Single Crystal at Elevated Temperature," *Kristall und Technik*., **13**, 791 (1978).

[71] B. Brenner and A. Luft, "The mechanism of Work Softening in Cold-Worked Molybdenum Polycrystals at an Elevated Temperature," *Mater. Sci. & Engi*., **52**, 229 (1982).
[72] T. Mori and M. Meshii, "Morphology of Plasticity and Dislocation Kinetics in Quenched Aluminum," Trans. JIM, 9, 96 (1968). T. Mori and M. Meshii, "Plastic Deformation of Quench-Hardened Aluminum Single Crystals," *Acta Metall*., **17**, 167 (1969).